

ADSORPTION AND INHIBITIVE CORROSION PROPERTIES OF NICOTINAMIDE ON CARBON STEEL IN COOLING WATER SYSTEMS

Florina BRANZOI^{a,*} and Viorel BRANZOI^b

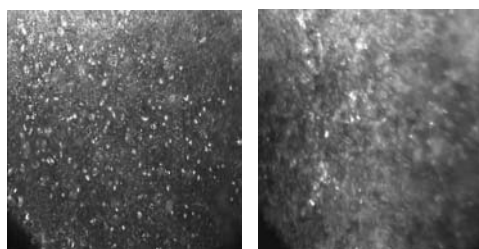
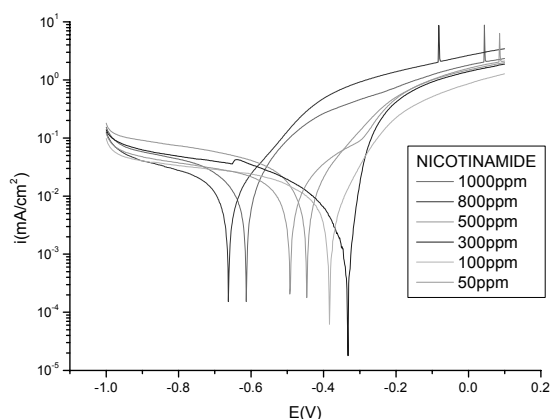
^a Institute of Physical Chemistry, 202 Splaiul Independenței, Bucharest 060021, Roumania

^b University Politehnica of Bucharest, Faculty of Applied Chemistry and Materials Science, 132 Calea Griviței, Bucharest, Roumania

Received December 20, 2013

Nicotinamide as organic inhibitor has anticorrosive properties and for this reason was used for cooling water systems protection. The inhibition activity analysis of this new organic inhibitor was made by assuming that the mechanism of inhibition by organic molecules is chemisorptions and that the energetic of the corrosion process per se is unaffected by the addition of substituents on the parent compound. We presume that this organic inhibitor, nicotinamide, inhibit corrosion of carbon steel by a protective mechanism, forming insoluble iron complexes and repairing the porous oxide layers. The methods employed were potentiodynamic polarization, electrochemical impedance spectroscopy, scanning electron microscopy (SEM) and metallurgical microscopy techniques. The addition of the organic inhibitors led in all the cases to inhibition of the corrosion process. The inhibition efficiency was high in all the studied cases. The corrosion parameters obtained from polarization curves and from EIS spectra are in good concordance and point out the inhibitory action of nicotinamide. The adsorptions of the organic compounds on the carbon steels surface obeyed Langmuir's isotherm. Further characterization using Fourier transform infrared spectroscopy (FT-IR) demonstrates the adsorption of organic inhibitors and the formation of corrosion products on the carbon steels surface.

The inhibition process was attributed to the formation of the adsorbed film on the metal surface that protects the metal against corrosive agents. The EIS measurements have confirmed this protection and pointed out the formation of adsorption layers on the electrode surface.



INTRODUCTION

Pure metals and alloys react chemically/ electrochemically with corrosive medium to form a stable compound, in which the loss of metal occurs. The compound so formed is called corrosion product and metal surface becomes corroded. Among the several methods of corrosion control and prevention, the use

of organic corrosion inhibitors is very well known.

The use of inhibitors is an important means to protect metallic materials against corrosion protection.¹⁻⁵ Different organic compounds containing nitrogen, oxygen and sulfur have been widely used as inhibitors. A literature survey shows that most of the organic inhibitors will act upon adsorption on the metal surface.⁶⁻⁸ The adsorption of inhibitors takes

* Corresponding author: fbrinzoi@chimfiz.icf.ro

place through heteroatoms such as nitrogen, oxygen, phosphorus and sulfur, triple bounds or aromatic rings and blocks the active sites decreasing the corrosion rates. The inhibition efficiency of organic inhibitor is mainly dependent on their affinity and compatibility to the metal surface.⁷⁻⁹

Metal corrosion in water-conveying systems such as cooling water circuits is of major concern in industrial applications. It is well known that in all the cases of cooling water systems at the metal/water surface contact appear frequent corrosion processes which determine deposition of corrosion products, like scales. Due to these scales formation the exchange heat becomes more difficult, fact that disturbs the normal function of industrial installation. In order to decrease corrosion of pipes, heat exchangers etc. corrosion inhibitors are widely applied.¹⁰⁻¹⁴

Many problems such as high cost of operation, compatibility with other chemicals, difficulty in understanding the cooling water systems, mechanism of inhibition, dosage of inhibitor required, arise in cooling water systems.⁹⁻¹¹

In the present work, the inhibition of carbon steel corrosion in cooling waters by Nicotinamide was investigated by potentiodynamic polarizations, EIS, FT-IR measurements and metallography analysis. This paper presents some attempts of analyzing the corrosive phenomena, which occur in cooling water systems, and relates to the protection of metallic surfaces from corrosion using these new polymers obtained in microwaves field.¹⁵⁻²²

EXPERIMENTAL

The inhibitory action was studied through tracing the polarization curves obtained using the potentiodynamic method, calculation of the corrosion kinetic parameters in case of solutions with inhibitors, especially the corrosion current densities, and their comparison with the kinetic parameters of the solution without inhibitors. The polarization curves were obtained by potentiostatic and potentiodynamic methods using a three electrode-cell. In all experiments the electrochemical polarizations were started about 30 minutes after the working electrode was immersed in solution, to allow the stabilization of the stationary potential. The working electrode potential was always measured with reference to the saturated calomel electrode and was plotted against current from external circuit, obtaining the anodic or cathodic curves according to the variation of the working electrode potential. The electrochemical impedance spectra were obtained in a frequency range from 100 kHz to 40 mHz. Disturbance amplitude of 10mV was applied relative to open circuit potential and ten measurements were performed for each frequency decade. The studied metals were the carbon steel type OL 37. The chemical compositions of the studied metallic materials are given in Table 1. The electrochemical measurements were made using an automated model VoltaLab 40 potentiostat/galvanostat. Surface analysis on the carbon steel electrode of the formed adsorbed film was accomplished by both FT-IR (FT-IR spectrometer Bruker optik) and metallographic micrographies (Hund H660).

The working electrode was carbon steel type OL 37 in the form cylindrical with an exposed area of 0.5 cm². Prior to each experiment the working electrode was polished successively with different grades of emery paper to 1200, 2500 and 4000, rinsed with bi-distilled water, degreased by acetone, washed thoroughly with bi-distilled water and dried at room temperature.

The corrosion medium was industrial cooling water type S1 with the chemical composition given in Table 2.

Table 1

The chemical composition of the working electrodes

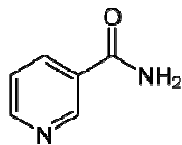
Electrode	C%	Si%	Mn%	Fe%	P%	S%	Al%	Ni%	Cr%	Cu%	Sn%	As%
OL 37	0.15	0.09	0.4	99.293	0.023	0.02	0.022	-	-	-	-	-

Table 2

The chemical composition of the cooling water type S1

Indicators	UM	Water type SC1 values of parameters
PH		8.42
Conductivity	μs/cm	1061
Alcalinity p	mval/L	0.1
Alcalinity m	mval/L	3.3
Total Hardness	mval/L	8.3
Calciu Hardness	mval/L	3.0
Chloride, Cl ⁻	mg/L	117.01
Sulfate	mg/L	155
Solid matters	mg/L	2.75
Organic matters	mg/L	11.37
Iron	mg/L	0.073
Aluminium,	mg/L	0.0175
Nitrite, NO ₂ ⁻	mg/L	<0.1
Nitrate, NO ₃ ⁻	mg/L	10
Phosphate, PO ₄ ³⁻	mg/L	0.046
Cuprum, Cu ²⁺	mg/L	<0.015
Zinc, Zn ²⁺	mg/L	<0.1

All tests have been performed at 25°C under atmospheric oxygen without agitation. The electrochemical measurements were made using an automated model VoltaLab 40 potentiostat/galvanostat. The used organic inhibitor was Nicotinamide.



Chemical molecular structure of the Nicotinamide.

RESULTS AND DISCUSSION

Fig. 1 depicts the anodic and cathodic polarization curves recorded on carbon steel OL-37 in cooling water system S1 with and without inhibitors at 25°C. Both anodic and cathodic curves were polarized in comparison with that obtained in the absence of inhibitor, thus inhibiting both the anodic dissolution of carbon steel and the reduction of hydrogen ions on the metal surface. This confirms that this inhibitor behave as a mixed inhibitor. The electrochemical parameters derived from the polarization curves at different concentrations are given in Table 3. This may be ascribed to adsorption of inhibitor over the corroded surface.

The values of corrosion current densities (i_{corr}), corrosion potential (E_{corr}), the cathodic Tafel slope (b_c), anodic Tafel slope (b_a), polarization resistance (R_p) and the inhibition efficiency ($E\%$) as function of Nicotinamide concentration were calculated from the curve 1 and given in Table 3.

Table 3 shows that the corrosion rate decreases obviously and efficiency increases with inhibitor concentrations. Analyzing Fig. 1 it can be observed that on the anodic curves there is a low active range of potential where the relation Tafel is verified. After this range the current densities slightly increases and tends to a limit value. This behaviour points out that on this range the corrosion process is controlled by diffusion. Sometimes on the anodic curves appear oxidation peaks followed by the narrow passive range and a decrease of the current density (this behaviour can be explained due to formation of oxo-hydroxo-complexes of Fe). The maximum efficiency is obtained at the inhibitor concentration of 300ppm and 100ppm for the system: Nicotinamide+OL37-S1. At the increasing inhibitor concentration over these concentrations (100 ppm and 300 ppm) the inhibitor efficiency starts to decrease, respectively the corrosion current densities begin to increase again.

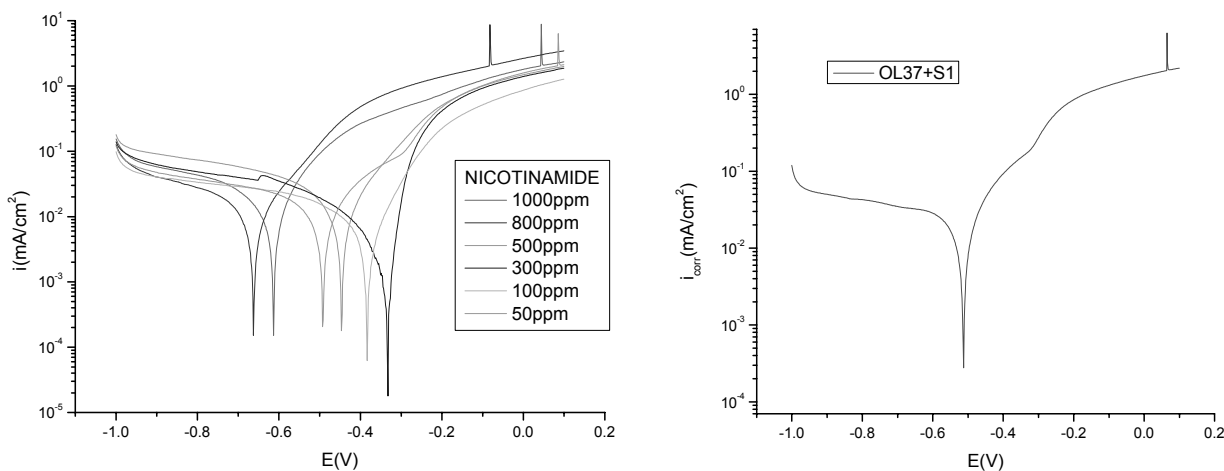


Fig. 1 – The polarization curves of OL 37 carbon steel in cooling water type S1 in presence and absence of Nicotinamide.

Table 3

Kinetic corrosion parameters of carbon steel OL-37 in cooling industrial water type S₁ in presence and absence of organic inhibitor type Nicotinamide at temperature of 25°C

Inhibitor (ppm)	i_{corr} ($\mu A/cm^2$)	R_p ($K\Omega/cm^2$)	R_{mpy}	$P_{mm/year}$	K_g (g/m^2h)	E (%)	E_{corr} (mV)	b_a (mV)	b_c (mV)	θ
0	13.01	1.78	6.07	0.15	0.137	-	-513	110	-215	
20	6.85	2.44	3.19	0.081	0.072	47	-586	80	-164	0.47
50	5.55	3.21	2.59	0.0657	0.0585	57	-495	99	-140	0.57
100	3.008	5.31	1.403	0.0356	0.0316	77	-385	78	-109	0.77
300	1.33	9.71	0.4307	0.0109	0.0097	89	-337	27	-71	0.89
500	5.41	2.90	2.57	0.0652	0.0580	60	-449	79	-133	0.60
800	5.54	2.96	2.58	0.0654	0.058	58	-664	95	-122	0.58
1000	6.25	2.52	2.91	0.07	0.065	52	-615	78	-126	0.52

Further, it was studied the influence of the immersion time of 500ppm Nicotinamide on the polarization behaviour of carbon steel in cooling water type S1. Because in Tables 3-4 are given synthetically all kinetic corrosion parameters, in Figs. 1-2 are presented only a few characteristic polarization curves for exemplification.

Effect of immersion time (1-196 h) on corrosion inhibition of Nicotinamide at 500 ppm concentration on the corrosion of OL37 in cooling water type S1 at 25°C was studied. Fig. 2 shows the anodic and cathodic polarization curves recorded on carbon steel OL-37 in cooling water system S1 obtaining in the presence of 500 ppm nicotinamide a function of time. It is noted that the corrosion rate increases with increasing the immersion time in presence of 500 ppm Nicotinamide (see Fig. 4a and Table 4). It is found that the inhibition efficiency of the inhibitor (500ppm Nicotinamide) decreases with increasing immersion time. This is due to desorption of inhibitor molecule with immersion time (see Fig. 4b and Table 4).

It is clear that the value of corrosion rate in the presence of 500 ppm Nicotinamide at 196 h is higher than that at 0 h or 1h time immersion.

The variation curves of the corrosion current density function of the 500 ppm Nicotinamide at different immersion times are presented in Fig. 2. From Fig. 2 and Table 4, one can see much better the influence of these parameters on the polarization behaviour of the carbon steel in cooling water system.

Analyzing in comparison Tables 3-4, it can be observed that the increase of inhibitor concentration led in all the cases to the decrease of the corrosion rate and once with the increase of the immersion time takes place a weakly decreasing of the inhibition efficiency and this fact can be explained on the basis of foregoing presented mechanism. We presume that once with increasing of the immersion time takes place an increasing of activity of: $Fe + OH^- \rightleftharpoons (FeOH)_{ads} + e^-$, $(FeOH)_{ads} \rightarrow (FeOH)^+ + e^-$, $(FeOH)^+ \rightarrow Fe^{2+} + OH^-$ and $[(FeOH)I_n]^+ \rightarrow [FeIn]^{2+} + OH^-$ and the inhibitor efficiency decreases slowly (see Tables 3-4).

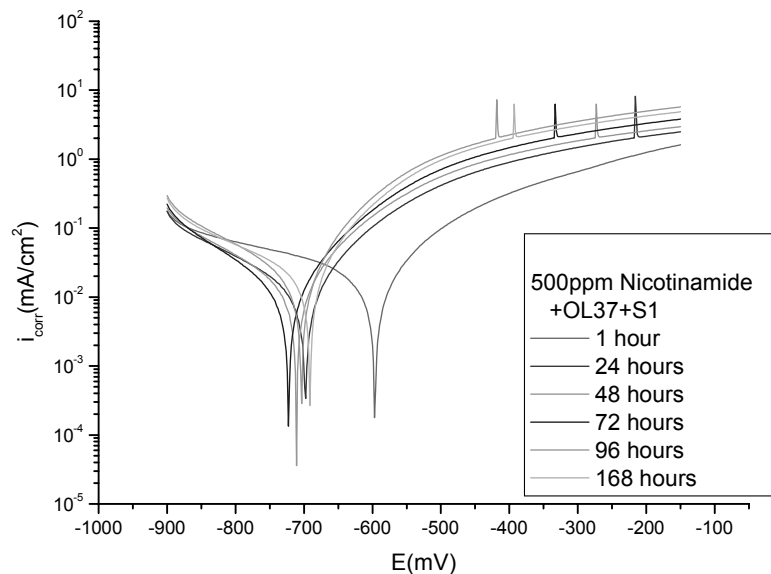


Fig. 2 – The polarization curves of OL 37 carbon steel in cooling water type S1 in presence of 500ppm Nicotinamide at different immersion times.

Table 4

Kinetic corrosion parameters of carbon steel OL-37 in cooling industrial water type S₁ in presence of 500ppm Nicotinamide at temperature of 25°C and different immersion times

time (h)	i_{corr} ($\mu A/cm^2$)	R_p ($K\Omega/cm^2$)	R_{mpy}	$P_{mm/year}$	K_g (g/m^2h)	E (%)	E_{corr} (mV)	b_a (mV)	b_c (mV)	θ
1	8.33	2.11	3.88	0.098	0.087	36	-599	78	-125	0.36
24	8.61	2.01	4.01	0.101	0.09	34	-701	82	-143	0.34
48	8.79	1.86	4.1	0.104	0.092	33	-712	77	-123	0.33
72	8.52	2.11	3.97	0.100	0.089	35	-742	81	-124	0.35
96	12.44	1.35	5.80	0.147	0.13	5	-704	67	-132	0.05
168	12.87	1.17	6.00	0.15	0.0135	2	-693	68	-153	0.02

The variation curves of the corrosion current density function of the inhibitor concentration and the influence of the inhibitor concentration with efficiency are presented in Fig. 3. The influence of immersion times of the inhibitor (500ppm Nicotinamide) on the corrosion rate of carbon steel

OL 37 in cooling water type S1 are presented in Fig. 4. From these figures, one can see much better the influence of these parameters on the polarization behaviour of the carbon steel OL 37 in cooling water system (S1).

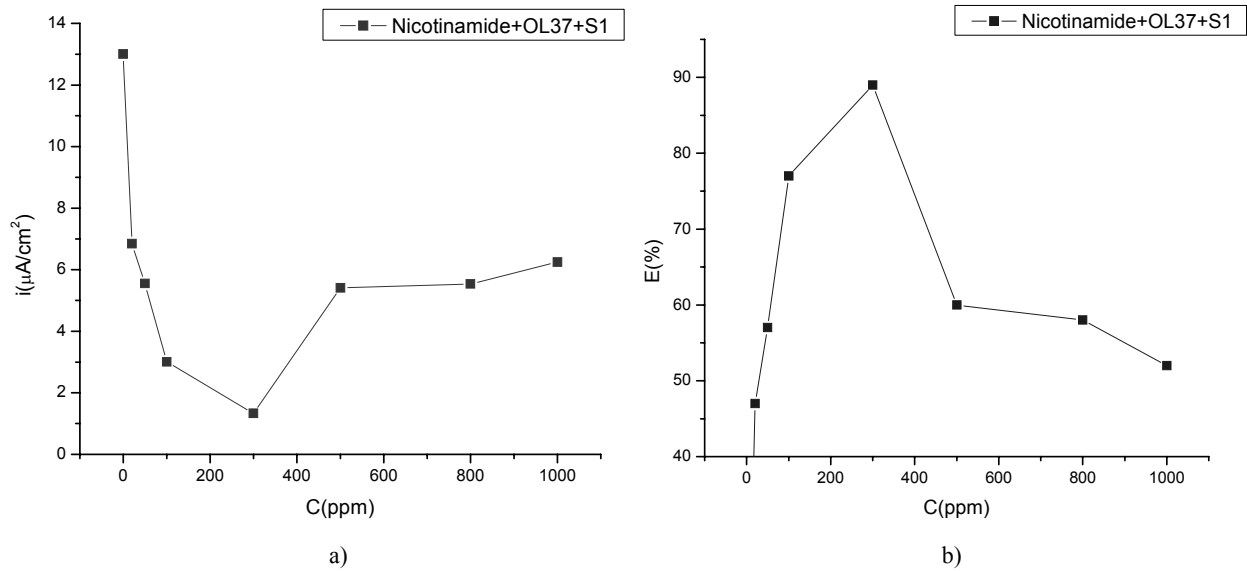


Fig. 3 – The influence of the inhibitor (Nicotinamide) concentration on the corrosion rate of carbon steel OL 37 in cooling water type S₁ (Fig. 3a) and the influence of the inhibitor concentration with efficiency (Fig. 3b) at a temperature of 25^oC.

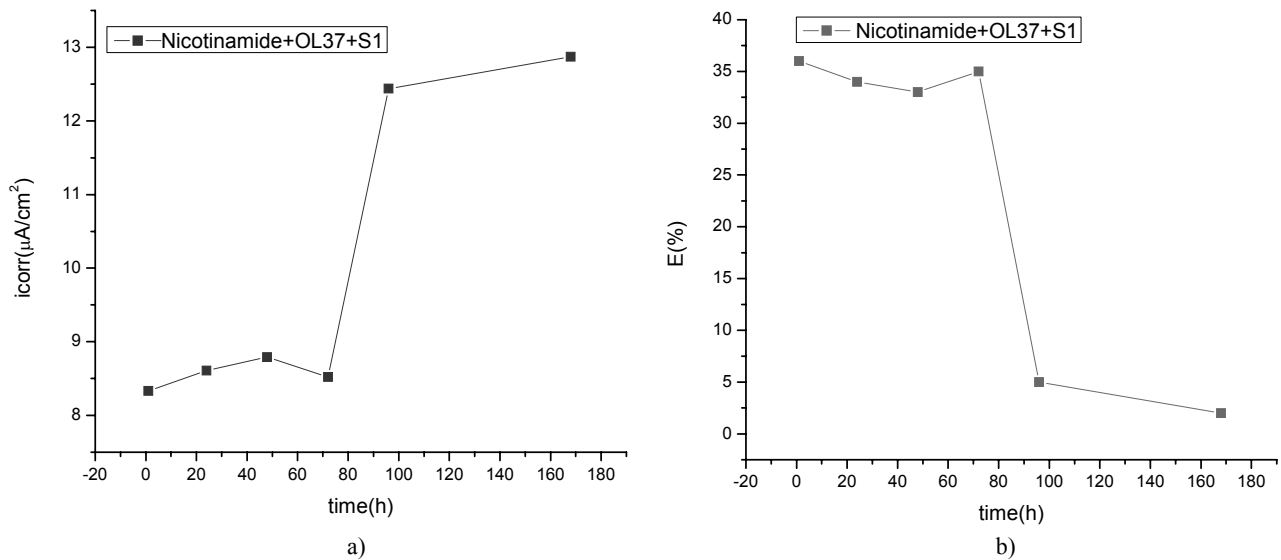


Fig. 4 – The influence of immersion times of the inhibitor (500ppm Nicotinamide) on the corrosion rate and efficiency of carbon steel OL 37 in cooling water type S₁.

Table 5

The values of K_{ads} and ΔG_{ads}° for studied systems

The system	Type of metallic material	Values of K_{ads} , M^{-1}	Values of ΔG_{ads}° KJM^{-1}	Type of adsorption
Cooling water type S ₁ +Nicotinamide	OL-37	0.938×10^4	-22.27	Physical adsorption and chemisorption

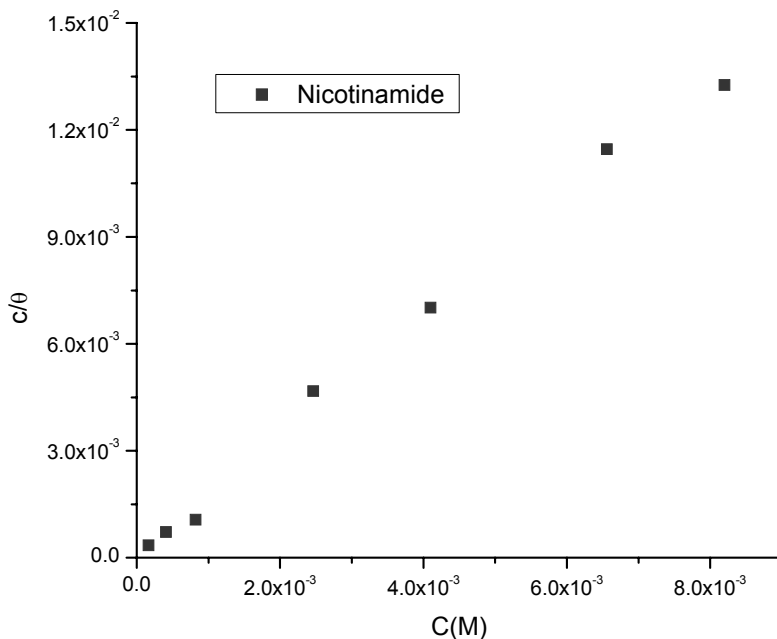


Fig. 5 – Langmuir plot for OL-37+Nicotinamide at different inhibitor concentrations and different immersion times.

We presume that the higher inhibitor efficiency is a consequence of the adsorption process. To quantify the effect of inhibitor concentration on the corrosion rate, it is common to fit the rate data to equilibrium adsorption expressions, such as Langmuir equation: $\theta / (1 - \theta) = KC$, where θ is the fraction of surface coverage by the inhibitor and K is the equilibrium constant for the adsorption reaction. θ is given by: $\theta = (i_{\text{corr}} - i_{\text{corr,inh}}) / i_{\text{corr}}$, where $i_{\text{corr,inh}}$ and i_{corr} are the corrosion rates in industrial cooling water S1 with and without inhibitor. Usage of the Langmuir treatment is often justified with the argument that inhibition must involve adsorption.

In this paper, the Langmuir isotherm is plotted against C , when a linear relationship is obtained for each inhibitor and a slope of near unity for each compound indicated approximate Langmuir behaviour (see Fig. 5). Further, we shall try to show what kind of adsorption process takes place on the electrode surface. The adsorption equilibrium constant (K_{ads}) is related to the standard free energy of reaction ($\Delta G_{\text{ads}}^{\circ}$) by the equation:

$$\ln K_{\text{ads}} = -(\Delta G_{\text{ads}}^{\circ} / RT) \quad (1)$$

The obtained values $\Delta G_{\text{ads}}^{\circ}$ up to -20KJmol^{-1} are consistent with electrostatic interaction between the charged molecules (in our case, the inhibitor molecules) and the charged metal surface (physical adsorption see Table 5), while those more negative than -40KJmol^{-1} , involve charge sharing or transfer

from the inhibitor molecules to the metal surface to form a co-ordinative type of bond (chemisorptions).

The corrosion of carbon steel in cooling water system S1 in the absence and presence of Nicotinamide were investigated by EIS. Electrochemical impedance measurements were performed at open circuit potential on the frequency range between 100 kHz and 40 mHz with an AC wave of $\pm 10 \text{mV}$ (peak-to-peak) and the impedance data were obtained at a rate of 10 points per decade change in frequency.

Nyquist plots for carbon steel obtained at the interface in the presence of inhibitor at optimum concentration are given in Fig. 6. All impedance spectra exhibit one capacitive loop and the diameter of the semicircles increases on increasing the inhibitor concentration suggesting that the formed inhibitive film was strengthened by the addition of inhibitors. However, these diagrams are not perfect semicircles and this fact is attributed to frequency dispersion.

The impedance spectra show a “depressed” semicircle. This phenomenon often referred to frequency dispersion of interfacial impedance has been attributed to the roughness, inhomogeneity of the solid surfaces and adsorption of inhibitor. The high and medium frequencies can be attributed to the charge transfer process and in the low frequencies can be attributed to the adsorption of corrosion products or adsorption of the inhibitor molecules on the carbon steel surface in cooling water with and without inhibitor.

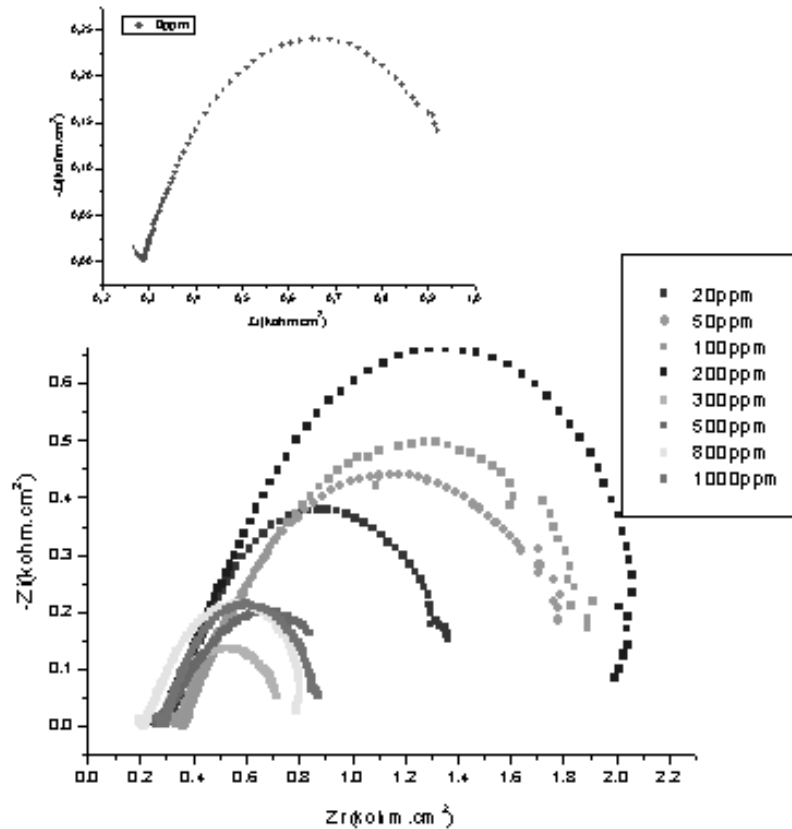


Fig. 6 – The Nyquist plot for OL37 in S1 with and without organic inhibitor.

The semicircular appearance shows that the corrosion of steel is controlled by charge transfer and the presence of inhibitor does not change the mechanism of dissolution. Figs. 6, 8 also indicate that the diameters of the capacitance loops in the presence of 200ppm Nicotinamide+OL37-S1, 300ppm and 100ppm Nicotinamide, and 500ppm Nicotinamide (after 1h and 24h immersion times) +OL37-S1 are bigger than those in the absence of organic inhibitors, suggesting that has good anticorrosion performance on the carbon steel in S1.

Bode diagrams presented in Figs. 7, 9 are in accordance with Nyquist diagrams. It can be observed that in absence of organic inhibitor the electrode presents one time constant at medium and low frequencies, this fact indicating an inductive behaviour with low diffusive tendency. On the contrary, in the presence of the organic inhibitor, the curve-phase angle versus log frequency appears a very well maximum defined which means that in this case the electrode has a good capacitive behaviour, according with the results obtained by electrochemical polarization and in concordance with the Nyquist diagrams.

All the obtained plots show only one semicircle and they were fitted using one time constant equivalent (see Fig. 10) mode with capacitance

(C), the charge transfer resistance (R_{ct}) and R_s solution resistance. The lower capacitance values for systems S1 +OL 37 with 100ppm, 300ppm and 500ppm Nicotinamide (after 1 h and 24 h immersion times), indicate the inhomogeneity of the metal surface roughened due to corrosion. The C_{dl} values decrease once with the increasing of the inhibitor concentration and reach very low values for the optimum concentrations of inhibitors for all the studied systems indicating the reduction of charges accumulated in the double layer due to the formation of adsorbed inhibitor layer.

In this paper, FT-IR spectrometry was used to identify whether there was adsorption and to provide new bonding information on the steel surface after immersion in the cooling water system containing organic inhibitor.²³⁻²⁷ All spectra in these experiments were obtained at a resolution 4 cm^{-1} in the region $650\text{-}4000 \text{ cm}^{-1}$.

The FT-IR spectra of pure organic inhibitor Nicotinamide is depicted in Fig. 11a and the FT-IR spectrum obtained for the carbon steel type OL 37, immersed in cooling water system type S1 containing 300ppm Nicotinamide organic inhibitor is presented in Fig. 11b and OL 37 in S1 containing 500ppm Nicotinamide is presented in Fig. 11c.

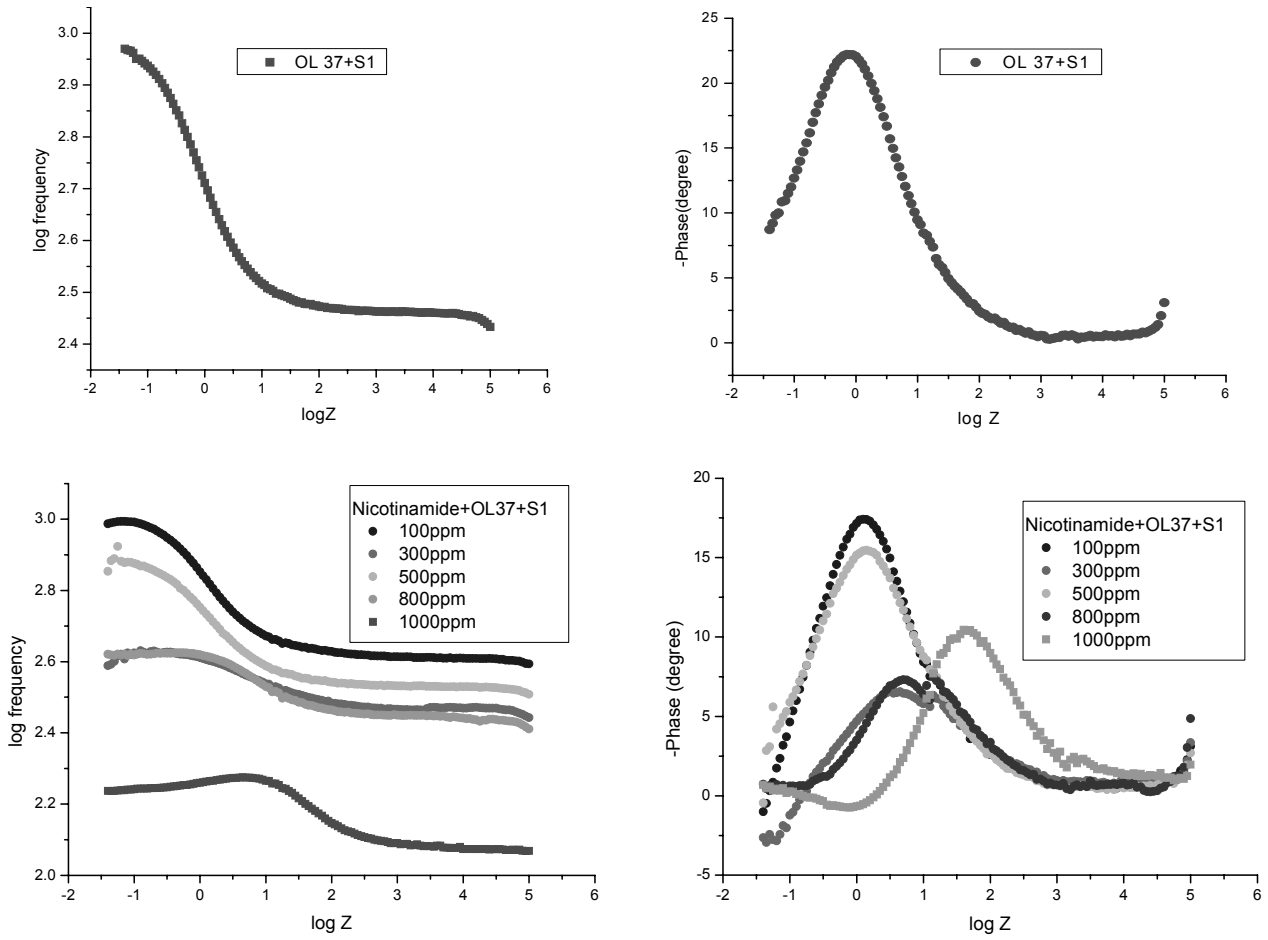


Fig. 7 – The Bode plot for OL37 in S1 with and without organic inhibitor.

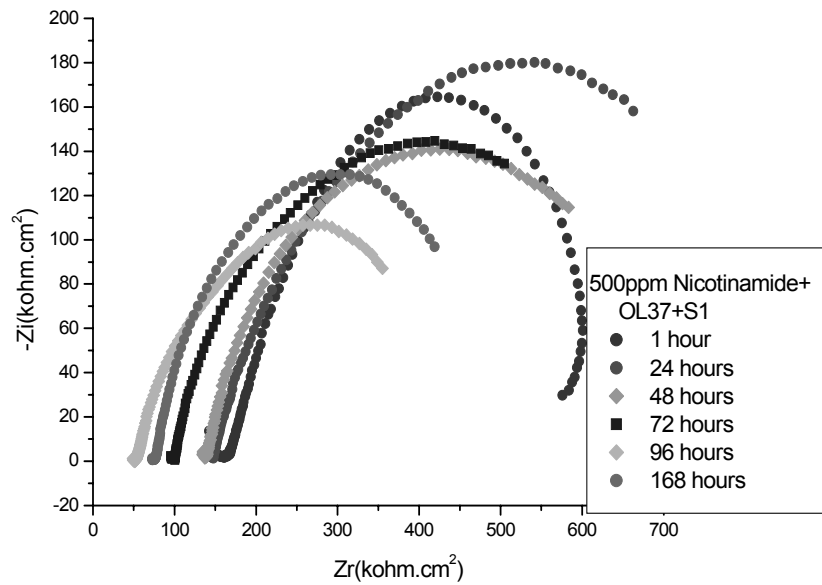


Fig. 8 – The Nyquist plot for OL37 in S1 with organic inhibitor and at different immersion times.

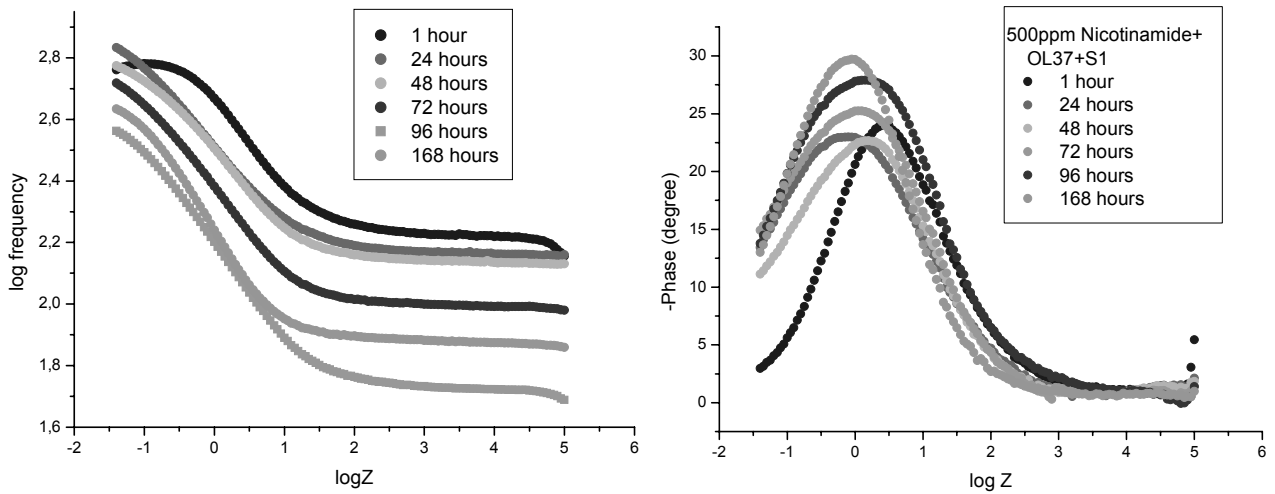


Fig. 9 – The Bode plot for OL37 in S1 with organic inhibitor and at different immersion times.

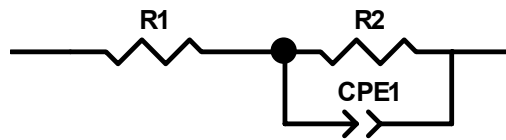


Fig. 10 – Equivalent circuit.

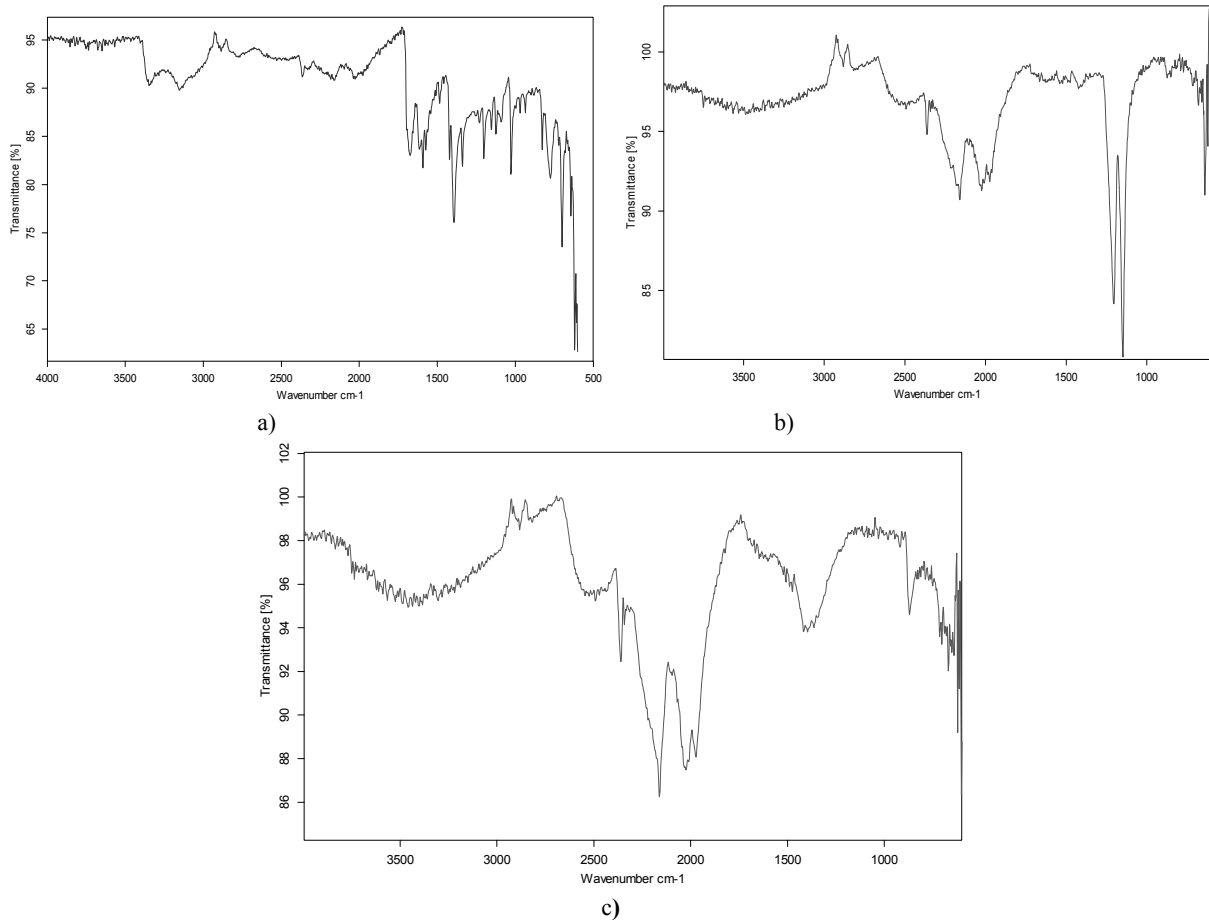


Fig. 11 – FT-IR spectra of (a) Nicotinamide, (b) OL 37+300 ppm Nicotinamide+ S1 and (c) OL37 +500 ppm Nicotinamide+ S1.

From Fig. 11a, a broad peak at 3350 cm^{-1} indicates the presence of the N-H bond of the Nicotinamide. The N-H in-plane bending vibrations usually occur in the region $1670\text{-}1590\text{ cm}^{-1}$. The weak band appears in the region $3150\text{-}3000\text{ cm}^{-1}$ due to C-H stretching vibrations. The bands for C-H in plane ring are bending vibrations in the region $1339\text{-}1000\text{ cm}^{-1}$ and the C-H out-of-plane bending

vibrations in the region $1090\text{-}643\text{ cm}^{-1}$. The presence of C-N stretching frequency is clearly manifest in the region $1673\text{ to }1592\text{ cm}^{-1}$. In this study, the C=O stretching vibrations is assigned at 1690 cm^{-1} and the C=O in-plane bending vibration is found at 700 cm^{-1} . In the present study, the C-NH₂ stretching vibration is observed at $1200\text{ and }1123\text{ cm}^{-1}$.

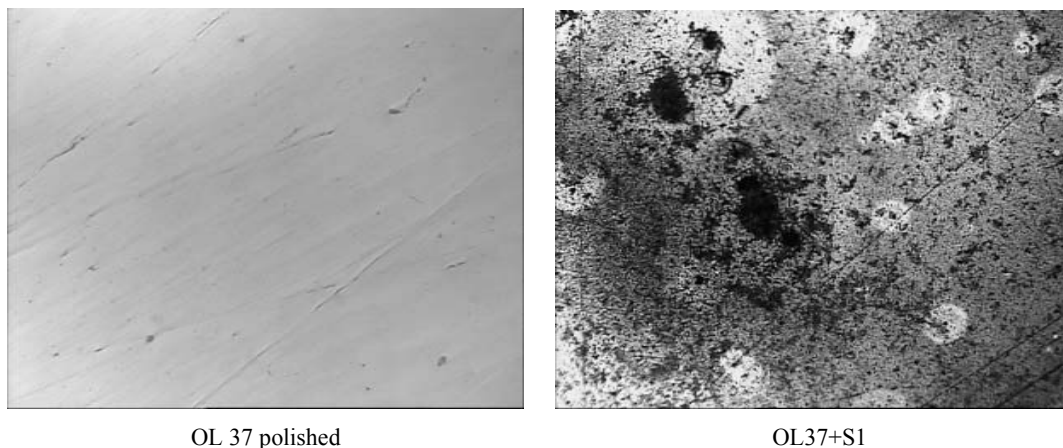


Fig. 12 – Micrographies of the carbon steel in cooling water S1: a) OL 37 polished, b) OL37+S1.

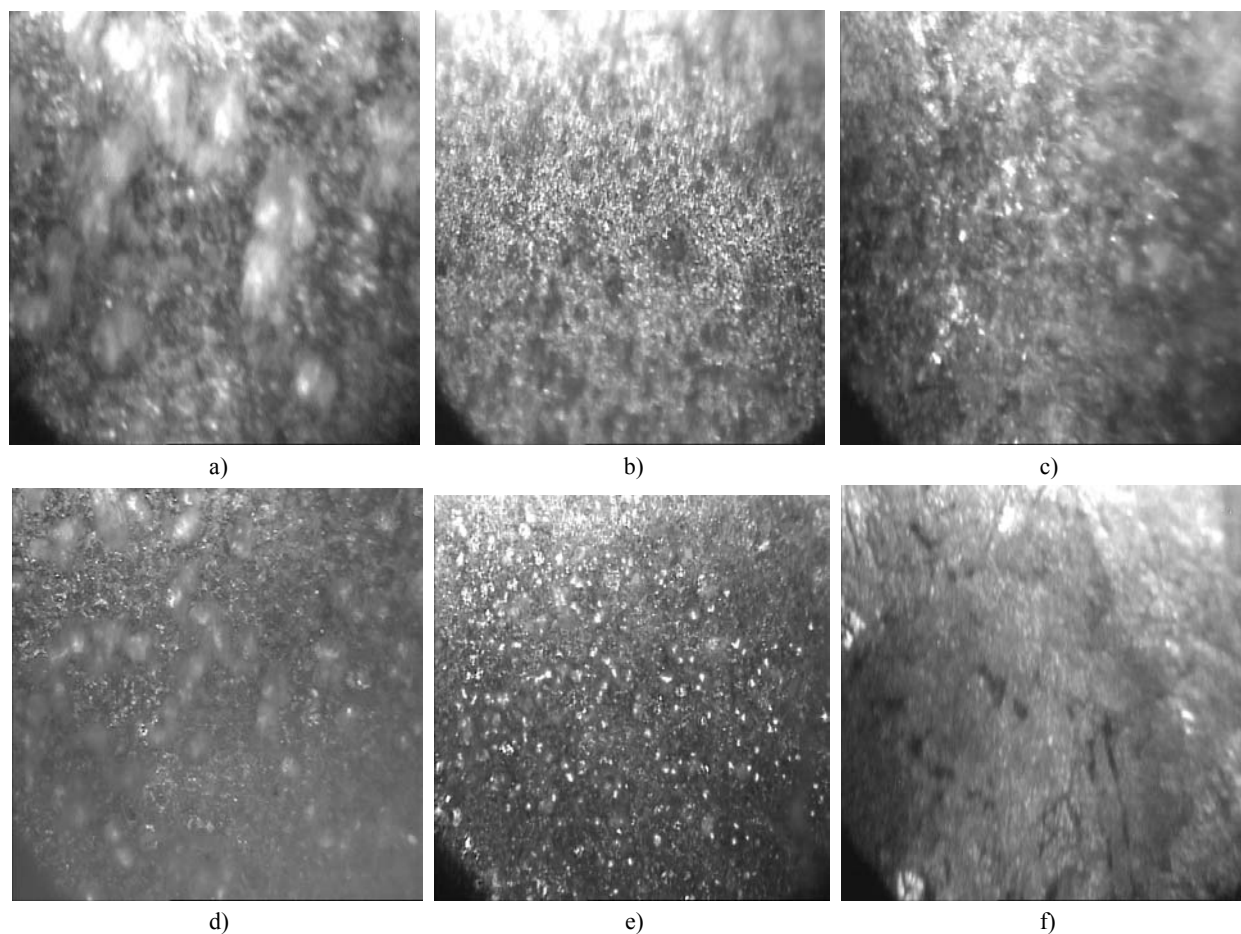


Fig. 13 – Micrographies of the carbon steel in cooling water S1 with organic inhibitor: a) OL37+100ppm Nicotinamide, b) OL37+300ppm Nicotinamide c) OL37+500ppm Nicotinamide d) OL37+800ppm Nicotinamide, e) OL37+500ppm Nicotinamide at 1h immersion time f) OL37+500ppm Nicotinamide at 72 h immersion time.

From Fig. 11b and 11c, a broad peak at 3306-3304 indicates the presence of the N-H bond of the OL37+S1+300ppm and 500ppm Nicotinamide. The N-H in-plane bending vibrations in the region 1680-1523 cm^{-1} . The weak band appears in the region 3050-3000 cm^{-1} due to C-H stretching vibrations. The bands for C-H in plane ring are bending vibrations in the region 1363-960 cm^{-1} and the C-H out-of-plane bending vibrations in the region 919-641 cm^{-1} . The presence of C-N stretching frequency is clearly manifest in the region 1680 to 1523 cm^{-1} . In this study, the C=O stretching vibration is assigned at 1646 cm^{-1} and the C=O in-plane bending vibration is found at 713 cm^{-1} . The presence of C-N stretching frequency is clearly manifested in the region 1416 to 1363 cm^{-1} . Moreover, these FT-IR measurements indicated at 3834 cm^{-1} the direct bonding between Fe atoms and Nicotinamide molecules via O and N atoms, and the formation Fe-inhibitor complex and this reveals that there is only chemical adsorption occurred on the surface of the metal.

Further, using the metallographic microscope the electrode surfaces were analyzed before and after a certain immersion in cooling water type S1. In Figs. 12-13 are given a few micrographies obtained for the following systems: carbon steel OL 37 after a certain immersion in cooling water type S1 with and without organic inhibitor. As it can be observed from Figs. 12-13 the corrosive attack is more accentuated in the cooling water system where the organic inhibitor concentration is lower than in the cases for which the organic inhibitor concentration is higher (see in comparison the micrographies from Figs. 12-13).²⁸⁻³⁰

Analyzing in comparison the Figs. 12-13, it can be observed that the corrosive attack is much more accentuated in the case of OL 37+ water type S1 system than in the case of OL-37+ water type S1 +Xppm inhibitor system. This finding is in good concordance with the results obtained by electrochemical method – see Tables 3-4 and the polarization curves from Figs. 1-2.

CONCLUSIONS

In the studied corrosion systems at low overvoltages, the corrosion process is under activation control, while at high overvoltages is controlled by diffusion.

The addition of organic inhibitors led in all the cases to the inhibition of the corrosion process.

The organic polymer which was obtained by us has presented a good inhibitory action and a significant efficiency for decreasing of the rate corrosion of the studied carbon steels.

The organic inhibitors were adsorbed on the carbon steel surface according to a Langmuir isotherm. The values of the adsorption constant determined from the plot of Langmuir isotherm pointed out that, in these cases there are physical adsorption.

FT-IR spectra revealed very clearly that the organic inhibitor Nicotinamide was adsorbed on the metal surface.

The adsorption of investigated organic inhibitor follows the Langmuir isotherm and the FT-IR results, also reveals the adsorption of inhibitor molecule on the metal surface and blocking the active sites.

EIS results are in very good concordance with results obtained by potentiodynamic and potentiostatic methods.

Nicotinamide inhibits both anodic and cathodic reactions by adsorption on the carbon steel surface and hence behave like mixed type inhibitor.

In all of the cases, the organic inhibitor type Nicotinamide in the systems OL37 in S1 had a good efficiency.

Acknowledgments: Financial support from National research Grant PN-II-32-137/2008 (Roumanian Ministry of Education and Research/CNMP) is gratefully acknowledged.

REFERENCES

1. H. H. Uhlig and R.W.Revie, "Corrosion and Corrosion Control", Wiley, New York, 3rd edition., 1985.
2. D. Jones, "Principle and Prevention of Corrosion", MacMillan Publishing Company, New York, 1992.
3. K. C. Pillai and R. Narayan, *J. Electrochem. Soc.*, **1978**, *125*, 1393.
4. J. L. Rozenfeld, "Corrosion Inhibitors", McGraw-Hill, New York, 1981, p.109.
5. V. Branzoi and F. Branzoi, *Rev. Roum. Chim.*, **2002**, *47*, 1193.
6. D. P. Schwensberg and V. Ashworth, *Corros. Sci.*, **1988**, *28*, 539.
7. V. Branzoi, F. Branzoi and L.Pilan, *Materials Chemistry and Physics*, **2009**, *118*, 197.
8. T. Hirai, J. Yamaki, T. Okada and A. Yamagi, *Electrochim. Acta*, **1985**, *30*, 61.
9. D. G. Leaist, *J. Chem. Soc. Faraday Trans.*, **1990**, *86*, 3487.
10. E. Kamis, F. Bellucci, R. M. Latonision and E. S. H. El-Ashry, *Corrosion*, **1991**, *47*, 677.
11. M. Beier and J. W. Schultze, *Electrochim. Acta*, **1992**, *37*, 2299.
12. F. Donahue and K. Nobe, *J. Electrochemical. Soc.*, **1965**, *112*, 886.
13. Y. A. Aleksanyan, I. I. Rformatskaya and A. N. Podobaev, *Protection of Metals*, **2007**, *43*, 125.

14. E. M. Sherif and S.-M. Park, *Electrochim. Acta*, **2006**, *51*, 4665.
15. M. J. Incorvia and S. Contarini, *J. Electrochem. Soc.*, **1989**, *136*, 2493.
16. F. Mansfeld, "Corrosion Mechanism", Marcel Dekker (Ed.), New York, 1987, p. 119.
17. V. Branzoi, F. Branzoi and L. Pilař, *Molec. Crystal & Liquid Crystals*, **2006**, *446*, 305.
18. G. Banerjee and S. N. Malhotra., *Corrosion*, **1992**, *48*, 10.
19. V. Branzoi, A. Pruna and F. Branzoi, *Rev. Roum. Chim.*, **2007**, *52*, 587.
20. K. Aramaki, J. Uehre and H. Nishihara, *Proc. of the 11th International Corrosion Congress*, Florence, Italy, **1990**, *3*, 331.
21. G. B. Hunt and A. K. Holiday, *Organic Chemistry*, **1981**, *14*, 229.
22. R. D. Braun, E. E Lopez and D. P. Vollmer, *Corros. Sci.*, **1993**, *34*, 1251.
23. H.W. Shen and Z.S Smialowsky., *Corrosion Sci.*, **1989**, *45*, 720.
24. A. Loupy, *Chemistry Today*, **2006**, *24*, 36.
25. Q. Qu, S. Jiang, W. Bai and L. Li, *Electrochim. Acta*, **2007**, *52*, 6811.
26. Q. Quing, L. Li, S. Jing and Z. Ding, *J. Appl. Electrochem.*, **2009**, *39*, 569.
27. M. F. L. Granero, P. H. L. S. Matai and I. C. Guedes, *J. Appl. Electrochem.*, **2009**, *39*, 1199.
28. D. Gopi, K. M. Govindaraju and L. Kavitha, *J. Appl. Electrochem.*, **2010**, *40*, 1349.
29. A. Prunã, V. Branzoi and F. Branzoi, *Materials and Technologies*, **2007**, *23*, 233.
30. F. Branzoi, V. Branzoi and I. Harabor, *Rev. Roum. Chim.*, **2011**, *56*, 115.